Communication

Direct Measurement of Tertiary Contact Cooperativity in RNA Folding

Bernie D. Sattin, Wei Zhao, Kevin Travers, Steven Chu, and Daniel Herschlag

J. Am. Chem. Soc., **2008**, 130 (19), 6085-6087 • DOI: 10.1021/ja800919q • Publication Date (Web): 23 April 2008

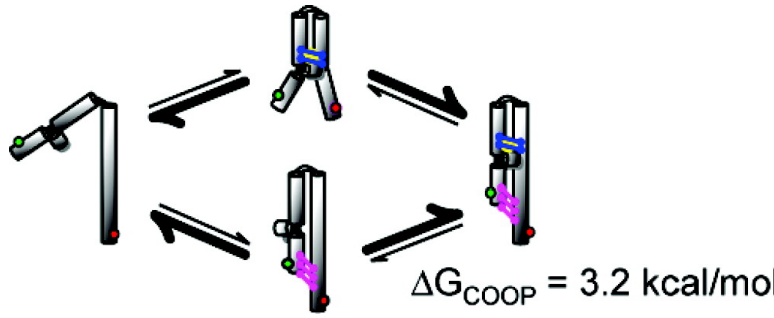

More About This Article

Additional resources and features associated with this article are available within the HTML version:

- Supporting Information
- Links to the 2 articles that cite this article, as of the time of this article download
- Access to high resolution figures
- Links to articles and content related to this article
- Copyright permission to reproduce figures and/or text from this article

View the Full Text HTML

J|A|C|S
COMMUNICATIONS

Published on Web 04/23/2008

Direct Measurement of Tertiary Contact Cooperativity in RNA Folding

Bernie D. Sattin,[†,‡] Wei Zhao,[‡] Kevin Travers,[†] Steven Chu,[‡,§] and Daniel Herschlag*[,†]

Departments of Biochemistry and Applied Physics, Stanford University, Stanford, California 94305, and Directorate, Lawrence Berkeley National Laboratory, Berkeley, California 94720

Received February 5, 2008; E-mail: herschla@stanford.edu

Cooperativity is a central feature of the structure and function of biological macromolecules. It is observed in the folding of proteins to their functional states, in the sharp response of hemoglobin and other proteins to changes in ligand concentration, and in the assembly of macromolecular complexes.

Cooperativity in domain formation during protein folding has evolved as a mechanism by which Nature overcomes the difficulty in selectively stabilizing a uniquely folded and functional structure (or small family of structures), among the vast number of partially folded and nonfunctional states that would likely dominate if each of the weak long-range domain contacts were to form independently. This thermodynamic scenario is well-documented for single domain proteins (e.g., refs 1–3) and is typically measured using double mutant cycles, analogous to the mutant cycle shown in Figure 1c.

Despite its fundamental importance, cooperativity is not always employed in all aspects of protein folding. Regions of proteins often form and break up as units, and these units are sometimes referred to as domains. Further, the cooperativity between domains can vary, from high, for a protein with extensive interfaces and reinforcing interactions,[4] to nonexistent, for a protein like titin with individual domains that are noninteracting "beads on a string".[5]

RNA, like proteins, must often fold to distinct three-dimensional structures to carry out biological functions. However, RNA forms stable secondary structure in the absence of tertiary structure, indicating some limits to cooperativity in RNA tertiary folding. Indeed, one might consider folding of an RNA from a preformed secondary structure to a functional tertiary structure as akin to folding of a multidomain protein. The fundamental question then arises: To what extent is there cooperativity in RNA folding?

We determined the tertiary contact cooperativity for the independently folding P4−P6 domain derived from the *T. thermophila* group I intron[6] (Figure 1a,b) using a single molecule fluorescence energy transfer (smFRET) folding assay. The P4−P6 crystal structure in 1996 revealed, for the first time, the side-by-side packing of RNA helices.[7] These helices are connected by a junction (J5/5a) and joined by two regions of tertiary contact, the metal core/metal core receptor (MC/MCR, Figure 1a,b, blue) and the tetraloop/tetraloop receptor (TL/TLR, Figure 1a,b, magenta).[6–10] We refer to these regions as "tertiary contacts", and we quantitatively investigate the energetic crosstalk between these tertiary contacts.

A thermodynamic scheme for determining the tertiary contact cooperativity in P4−P6 is shown in Figure 1c. The unfolded

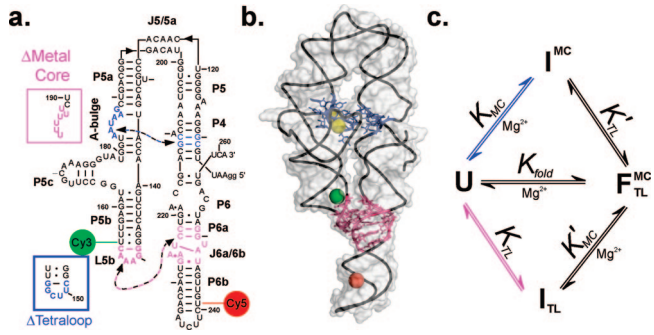

Figure 1. Molecular constructs and energetic scheme for measuring cooperativity in P4−P6. The P4−P6 secondary structure (a) and crystal structure (b), with the metal core/metal core receptor (blue, with yellow Mg^{2+} ions) and tetraloop/tetraloop receptor (magenta) highlighted. Each P4−P6 construct was internally dye-labeled with Cy3 at U155 (green), with Cy5 at U241 (red), and extended by 26 nucleotides at the 3′-end to provide a surface tether for single molecule experiments. To measure tertiary contact cooperativity using the thermodynamic scheme shown in (c), a metal core ablation mutant (ΔMetal Core) and tetraloop ablation mutant (ΔTetraloop) were constructed, and the folding of these mutants and wild-type P4−P6 was followed (eq 1). The A-bulge was mutated to uridine residues to ablate the metal core, and the GAAA tetraloop was mutated to UUCG to ablate the tetraloop (a). The wild-type construct was used to measure the overall stability of P4−P6, K_{fold}; the ΔMetal Core construct was used to measure the stability of the tetraloop/tetraloop receptor interaction alone, K_{TL}, and the ΔTetraloop construct was used to measure the stability of the metal core/metal core receptor interaction alone, K_{MC}.

ensemble (U) comprises the large number of conformations with secondary structure but no tertiary contacts. The unfolded ensemble is in equilibrium with the fully folded state F^{MC}_{TL}, which has both tertiary contacts formed, and this equilibrium is described by K_{fold}. The two intermediate species, I_{TL} and I^{MC}, have only one tertiary contact formed. In I_{TL}, the tetraloop/receptor contact is formed (L5b docked into J6a/6b; Figure 1a,b, magenta), and in I_{MC}, the metal ion core/receptor is formed[11] (folded P5abc subdomain with the A-rich bulge (A-bulge) docked into P4; Figure 1a,b, blue).

To determine the equilibrium constants for the thermodynamic cycle of Figure 1c, we internally dye-labeled the wild-type molecule and two known tertiary contact ablation mutants: a metal core ablation mutant (ΔMetal Core) in which the A-bulge is mutated to uracil residues, preventing formation of the MC/MCR contact,[10] and a tetraloop ablation mutant (ΔTetraloop) in which the GAAA tetraloop is mutated to a UUCG tetraloop, preventing docking to the tetraloop receptor[10,12–14] (Figure 1). These mutations selectively disrupt individual tertiary contacts without detectably altering the structure of the other tertiary contact, as evidenced by previously determined hydroxyl radical footprinting protection patterns.[10] The constructs were labeled with Cy3 and Cy5 such that the dyes are predicted to be within

[†] Department of Biochemistry, Stanford University.
[‡] Department of Applied Physics, Stanford University.
[§] Lawrence Berkeley National Laboratory.

~4 nm of one another in the folded state and distant (>10 nm) in the unfolded states (Figure 1a,b). Molecules were attached to a BSA-biotin/streptavidin-coated quartz surface via hybridization to a biotinylated DNA tether.[15,16]

To detect any adverse effects of dye labeling and/or surface tethering, the Mg^{2+}-dependent folding transition was followed and compared to that observed for free, unlabeled, untethered P4−P6 obtained by solution chemical protection. The folding transitions measured by smFRET and hydroxyl radical footprinting were the same for each construct (WT: $[Mg^{2+}]_{1/2}$ = 2.6 ± 0.2 and 2.4 ± 0.1 mM (smFRET and footprinting, respectively); ΔMetal Core: $[Mg^{2+}]_{1/2}$ = 18 ± 4 and 13.5 ± 1.4 mM; ΔTetraloop: $[Mg^{2+}]_{1/2}$ = 41 ± 4 and 41 ± 7 mM; see Supporting Information).

The smFRET data show that the three dye-labeled P4−P6 constructs stochastically fluctuate between two FRET states (Figure 2a). The WT (black) and ΔMetal Core (magenta) constructs fluctuate between FRET levels of 0.1 and 0.8, and the ΔTetraloop construct fluctuates between FRET levels of 0.1 and 0.5 (blue). The FRET levels remain the same for each construct as the concentration of Mg^{2+} is increased despite the higher fraction of time spent in the high FRET state at higher Mg^{2+} (Supporting Information and data not shown). These results, as well as experiments with varying time resolution (8−25 ms, data not shown), indicate that FRET averaging from rapid exchange between states does not occur between the folded and unfolded states so that the observed FRET values reflect those for the unfolded and folded states.[16,17]

As K_{TL} represents the formation of the TL/TLR contact without the MC/MCR contact preformed and K'_{TL} the formation of the contact with the MC/MCR contact preformed (Figure 1c), the ratio of these two equilibrium constants can be used to calculate the tertiary contact cooperativity, ΔG_{coop}, as described in eq 1, which is derived from Figure 1c; that is, how much the formation of one contact favors formation of the other.

$$\Delta G_{coop} = -RT \ln (K'_{TL}/K_{TL}) = -RT \ln (K'_{MC}/K_{MC}) \quad (1)$$
$$= \Delta G'_{TL} - \Delta G_{TL} = \Delta G'_{MC} - \Delta G_{MC}$$

The analogous relationship also holds for the MC/MCR contact, as is also shown in eq 1, and ΔG_{coop} is the same when calculated for either contact because the equilibria are related to one another within the thermodynamic cycle of Figure 1c.

We measured the stability of all three P4−P6 constructs under identical conditions to obtain the equilibrium contants needed to determine ΔG_{coop} (10 mM $MgCl_2$, 200 mM NaCl, 50 mM NaMOPS, 22 °C, pH 7.0). The wild-type strongly favored the high FRET state such that the fraction of time spent in that state was 92 ± 1% (Figure 2b, black). In contrast, the two mutants strongly favored the low FRET state. For the P4−P6 ΔMetal Core construct, the fraction of time spent in the high FRET state was 33 ± 1% (Figure 2b, magenta), while for the P4−P6 ΔTetraloop construct, the fraction of time spent in the high FRET state was 9 ± 1% (Figure 2b, blue). The favorable folding of wild-type and unfavorable folding of the mutants qualitatively indicates that there is cooperativity between the two tertiary contacts.

A quantitative measure of cooperativity was obtained from the equilibrium constants for the wild-type and mutant RNAs and applied in Figure 1c, as shown in Figure 2b. The equilibria between U, I_{MC}, and F_{TL}^{MC} (K_{MC}, K_{fold}, and K'_{TL}) constitute a thermodynamic cycle such that the measured equilibrium constants can be used to calculate the stability of the tetraloop

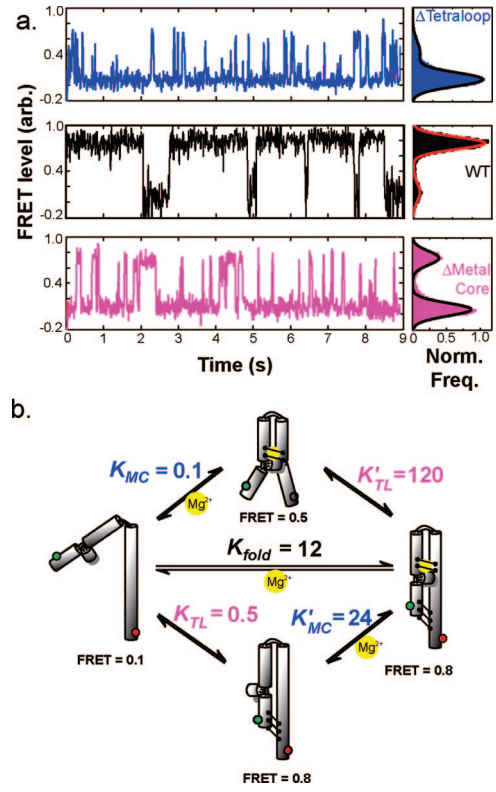

Figure 2. Three equilibrium distributions, measured by single molecule FRET, to determine tertiary contact cooperativity in P4−P6 RNA. Sample of single molecule FRET traces and cumulative distribution histograms (a) of the tetraloop ablation (ΔTetraloop, blue), the wild-type (WT, black), and the metal core ablation (ΔMetal Core, magenta) constructs under identical conditions (10 mM $MgCl_2$, 200 mM NaCl, 50 mM NaMOPS, 22 °C, pH 7.0). The relative populations of low and high FRET states were determined by Gaussian fitting of the two FRET peaks (black or red lines). The ΔTetraloop molecules spend 9 ± 1% (K_{MC} = 0.10 ± 0.01) of the time in the high FRET state, the WT molecules spend 92 ± 1% (K_{fold} = 12 ± 1) of the time in the high FRET state, and the ΔMetal Core molecules spend 33 ± 1% (K_{TL} = 0.50 ± 0.02) of the time in the high FRET state. (b) The tertiary cooperativity scheme, with cartoons to depict structures of P4−P6 based on observed FRET values. Assuming a standard dependence of FRET level on dye proximity, the dye pair is at least 10 nm apart in the unfolded ensemble (U). In the folded state and I_{TL}, the dye pair is estimated to be ~4 nm apart, the expected proximity of the pair with the tetraloop/tetraloop receptor formed. The I_{MC} intermediate has a lower FRET value of 0.5 (independent of $[Mg^{2+}]$, see Figure S1). The measured equilibrium constants, obtained from {(Frac High FRET)/(Frac Low FRET)} and the thermodynamic cycle in (b), were used to determine K'_{TL} = 120 and K'_{MC} = 24.

with the metal core preformed, $K'_{TL} = K_{fold}/K_{MC}$ = 12/0.1 = 120 (Figure 2b); similarly, a thermodynamic cycle between U, I_{TL}, and F_{TL}^{MC} gives K'_{MC} = 24 (Figure 2b). These results allow quantitation of the tertiary cooperativity according to eq 1. In each case, tertiary contact formation is 240-fold more favorable subsequent to formation of the other tertiary contact (K'_{TL}/K_{TL} = 120/0.5 = K'_{MC}/K_{MC} = 24/0.1 = 240), corresponding to a tertiary cooperativity of 3.2 ± 0.2 kcal/mol.

The magnitude of the cooperativity measured here for RNA folding is comparable to what is found in protein folding (e.g., refs 4 and 18), although it is not clear if the mechanistic underpinnings are the same. Most generally, the presence of thermodynamic cooperativity in folding indicates the presence of an energetic barrier to the formation individual long-range interactions that, once overcome, need not be surmounted again. In protein folding, this barrier has been attributed to the energetic penalty for the conformational restriction paid to form a single long-range contact and to the rather precise fit of packed side

chains in the fully folded state that maximizes van der Waals packing and minimizes the solvation penalty for exposed hydrophobic groups, relative to partially folded states.

In RNA folding, the physical origins of cooperativity are likely to include an electrostatic component derived from the electrostatic penalty for bringing two highly negatively charged coaxially stacked helices (e.g., P456 and P5abc) together in space. Indeed, smFRET experiments with lower concentrations of screening cations reveal greater cooperativity (unpublished results), consistent with the presence of an electrostatic barrier that contributes to the observed cooperativity.

The assembly of macromolecular structure to populate a single state (or small family of states) can occur without significant cooperativity between tertiary contacts; that is, the stability of individual tertiary contacts can be independent of the presence of additional tertiary contacts. In larger RNAs, where the tertiary contacts are more distant, this may be common. Further exploration of cooperativity in RNA folding is needed. Such experiments will help reveal similarities and distinctions between RNA and protein folding and will further our understanding of this fundamental feature of biological macromolecules.

Surprisingly, the number of RNA systems in which cooperativity has been rigorously dissected is limited.[19,20] Indeed, quantitative energetic dissection of the cooperativity underlying formation of RNA tertiary structure has remained difficult for experimental and conceptual reasons. Tertiary contact ablations,[21] or even single-point mutations,[15,22] often result in large shifts in Mg^{2+}-dependent RNA folding. Because equilibrium measurements are inaccurate away from the Mg^{2+} midpoint, data have typically been fit by a Hill equation to extrapolate folding equilibria to a common Mg^{2+} concentration. However, this extrapolation requires an assumption that folding involves a transition from the same unfolded to the same folded state under all conditions, that is, a two-state assumption. This assumption is unlikely to hold for RNA because its polyelectrolyte nature results in a different constellation of associated ions at each Mg^{2+} concentration and, in particular, for the unfolded state, a different ensemble of unfolded conformers.[23–26] This extrapolation gives an estimate for P4−P6 folding cooperativity of 4.6 ± 0.5 kcal/mol instead of the value of 3.2 ± 0.2 kcal/mol obtained herein (see Supporting Information). Indeed, some extrapolations of energetic effects from mutations have given calculated $\Delta\Delta G$ effects for single-point mutants of >10 kcal/mol (e.g., refs 21, 23), values that likely greatly overestimate the actual energetic differences.

SmFRET experiments avoid this pitfall because the high accuracy achievable in measurement of equilibria well away from a folding midpoint[15,22] allows direct comparison of equilbria under identical conditions. For example, in bulk, a 5% folding signal may be difficult to distinguish from, for example, a 3% signal; in the corresponding smFRET experiment, the folding signal is 100% (for 5% of the time), making determination of the amount of folded molecule present straightforward. Interpretation of the bulk experiment is further complicated because the signal for an unfolded ensemble often varies with conditions, a phenomenon that is sometimes referred to as "sloping baselines" and is often a manifestation of the non-two-state behavior of these systems. Thus, a 5% bulk signal can represent 5% of the molecules in the folded state or differences in the predominant conformation(s) of the unfolded ensemble. Again, this scenario can be readily distinguished from a small population of folded molecules in smFRET experiments because the FRET signal of the states that are populated are directly reported. We expect smFRET experiments to be key in dissecting the energetic underpinnings of RNA structure assembly and testing the underlying molecular origins of folding cooperativity.

Acknowledgment. We thank Tae-Hee Lee and Harold Kim for providing instrumental expertise, Yunxiang Zhang for help with data processing, Nathan Boyd for experimental assistance, Jan Lipfert and members of the Herschlag lab for helpful discussions comments on the manuscript. B.D.S. was supported by the Stanford Quantitative Chemical Biology Program (NIH DK071499) and is currently a Leukemia and Lymphoma Society Fellow. This work was supported by an NIH Program Project Grant (P01-GM-066275) to D.H. and S.C. and, in part, by grants from the NSF and DARPA to S.C.

Supporting Information Available: Experimental procedures; Mg^{2+} titrations of all three constructs performed by hydroxyl radical footprinting and by smFRET; and cumulative distributions of the ΔTL construct at increasing [Mg^{2+}]. This material is available free of charge via the Internet at http://pubs.acs.org.

References

(1) Faisca, P. F.; Plaxco, K. W. *Protein Sci.* **2006**, *15*, 1608–1618.
(2) Onuchic, J. N.; Luthey-Schulten, Z.; Wolynes, P. G. *Annu. Rev. Phys. Chem.* **1997**, *48*, 545–600.
(3) Shakhnovich, E. *Chem. Rev.* **2006**, *106*, 1559–1588.
(4) Batey, S.; Randles, L. G.; Steward, A.; Clarke, J. *J. Mol. Biol.* **2005**, *349*, 1045–1059.
(5) Scott, K. A.; Steward, A.; Fowler, S. B.; Clarke, J. *J. Mol. Biol.* **2002**, *315*, 819–829.
(6) Murphy, F. L.; Cech, T. R. *Biochemistry* **1993**, *32*, 5291–5300.
(7) Cate, J. H.; Gooding, A. R.; Podell, E.; Zhou, K. H.; Golden, B. L.; Kundrot, C. E.; Cech, T. R.; Doudna, J. A. *Science* **1996**, *273*, 1678–1685.
(8) Murphy, F. L.; Cech, T. R. *J. Mol. Biol.* **1994**, *236*, 49–63.
(9) Uchida, T.; He, Q.; Ralston, C. Y.; Brenowitz, M.; Chance, M. R. *Biochemistry* **2002**, *41*, 5799–5806.
(10) Takamoto, K.; Das, R.; He, Q.; Doniach, S.; Brenowitz, M.; Herschlag, D.; Chance, M. R. *J. Mol. Biol.* **2004**, *343*, 1195–1206.
(11) Folding to form F and I^{MC} occurs from an unfolded ensemble with the Mg^{2+} ions of the metal ion core (in P5abc) bound. In contrast, folding to form I_{TL} occurs from an unfolded state without those metal ions bound. We assume that metal ion binding does not affect TL/TLR stability.
(12) Jaeger, L.; Michel, F.; Westhof, E. *J. Mol. Biol.* **1994**, *236*, 1271–1276.
(13) Treiber, D. K.; Williamson, J. R. *J. Mol. Biol.* **2001**, *305*, 11–21.
(14) Shcherbakova, I.; Brenowitz, M. *J. Mol. Biol.* **2005**, *354*, 483–496.
(15) Zhuang, X. W.; Bartley, L. E.; Babcock, H. P.; Russell, R.; Ha, T. J.; Herschlag, D.; Chu, S. *Science* **2000**, *288*, 2048–2051.
(16) Kim, H. D.; Nienhaus, G. U.; Ha, T.; Orr, J. W.; Williamson, J. R.; Chu, S. *Proc. Natl. Acad. Sci. U.S.A.* **2002**, *99*, 4284–4289.
(17) Joo, C.; McKinney, S. A.; Lilley, D. M.; Ha, T. *J. Mol. Biol.* **2004**, *341*, 739–751.
(18) Kloss, E.; Courtemanche, N.; Barrick, D. *Arch. Biochem. Biophys.* **2008**, *469*, 83–99.
(19) Doherty, E. A.; Herschlag, D.; Doudna, J. A. *Biochemistry* **1999**, *38*, 2982–2990.
(20) Kieft, J. S.; Zhou, K.; Jubin, R.; Murray, M. G.; Lau, J. Y.; Doudna, J. A. *J. Mol. Biol.* **1999**, *292*, 513–529.
(21) Battle, D. J.; Doudna, J. A. *Proc. Natl. Acad. Sci. U.S.A.* **2002**, *99*, 11676–11681.
(22) Ha, T.; Zhuang, X. W.; Kim, H. D.; Orr, J. W.; Williamson, J. R.; Chu, S. *Proc. Natl. Acad. Sci. U.S.A.* **1999**, *96*, 9077–9082.
(23) Silverman, K. S.; Zheng, M. X.; Wu, M.; Tinoco, I.; Cech, T. R. *RNA* **1999**, *5*, 1665–1674.
(24) Misra, V. K.; Draper, D. E. *Proc. Natl. Acad. Sci. U.S.A.* **2001**, *98*, 12456–12461.
(25) Das, R.; Mills, T. T.; Kwok, L. W.; Maskel, G. S.; Millett, I. S.; Doniach, S.; Finkelstein, K. D.; Herschlag, D.; Pollack, L. *Phys. Rev. Lett.* **2003**, *90*, 188103.
(26) Das, R.; Travers, K. J.; Bai, Y.; Herschlag, D. *J. Am. Chem. Soc.* **2005**, *127*, 8272–8273.

JA800919Q